Chemical Therapeutics

Molecular Cancer Therapeutics

Designing and Developing S100P Inhibitor 5-Methyl Cromolyn for Pancreatic Cancer Therapy

Thiruvengadam Arumugam[1], Vijaya Ramachandran[1], Duoli Sun[2], Zhenghong Peng[2], Ashutosh Pal[2], David S. Maxwell[2], William G. Bornmann[2], and Craig D. Logsdon[1,3]

Abstract

We have previously shown that the antiallergic drug cromolyn blocks S100P interaction with its receptor receptor for advanced glycation end product (RAGE) and improves gemcitabine effectiveness in pancreatic ductal adenocarcinoma (PDAC). However, the concentration required to achieve its effectiveness was high (100 μmol/L). In this study, we designed and synthesized analogs of cromolyn and analyzed their effectiveness compared with the parent molecule. An ELISA was used to confirm the binding of S100P with RAGE and to test the effectiveness of the different analogs. Analog 5-methyl cromolyn (C5OH) blocked S100P binding as well as the increases in NF-κB activity, cell growth, and apoptosis normally caused by S100P. *In vivo* C5OH systemic delivery reduced NF-κB activity to a greater extent than cromolyn and at 10 times lesser dose (50 mg vs. 5 mg). Treatment of mice-bearing syngeneic PDAC tumors showed that C5OH treatment reduced both tumor growth and metastasis. C5OH treatment of nude mice bearing orthotopic highly aggressive pancreatic Mpanc96 cells increased the overall animal survival. Therefore, the cromolyn analog, C5OH, was found to be more efficient and potent than cromolyn as a therapeutic for PDAC. *Mol Cancer Ther; 12(5); 654–62. ©2013 AACR.*

Introduction

Pancreatic ductal adenocarcinoma (PDAC) is the fourth leading cause of cancer death in the United States and leads to an estimated 227,000 deaths per year worldwide (1, 2). There is no effective therapy for pancreatic cancer other than early resection (3). However, only 15% to 20% of patients are surgical candidates at the time of diagnosis (3). Gemcitabine has been the mainstay of systemic treatment for more than a decade but with a meager therapeutic benefit (4). Multiple chemotherapeutic and targeted agents have also been combined with gemcitabine without significant therapeutic benefit over gemcitabine alone (3, 4). However, recently many molecular abnormalities underlying pancreatic carcinogenesis and progression have been identified (5). This has stimulated the search for novel therapeutic approaches for this aggressive disease.

S100P is a 95–amino acid member of the S100 family of proteins that was first purified from placenta (6) and can act as both intracellular and extracellular signaling molecule (7). There is an increasing evidence suggesting that S100P has a significant role in cancer (7). This gene has been found to be expressed in several forms of the disease, including pancreas, breast, colon, prostate, and lung, and has been shown to be associated with poor clinical outcomes (8–12). S100P is secreted from cancer cells and acts extracellularly through the receptor for advanced glycation end products (RAGE; ref. 13). RAGE is a member of the immunoglobulin superfamily of cell surface molecules that is activated by multiple ligands (14). Acting through RAGE, S100P was shown to activate MAPkinase and NF-κB pathways in pancreatic cancer cell lines (7, 13). These 2 pathways are constitutively active in most pancreatic cancer cell lines, and influence tumor growth and chemotherapeutic drug resistance (15, 16). Apart from cancer cells, several cells in the tumor microenvironment such as endothelial, smooth muscle, fibroblast, and leukocytes including macrophages express RAGE (14). Recently it was shown that genetic deletion of RAGE inhibits the development and progression of PDAC and prolongs survival in a mouse model (12). Taken together, the evidence supports that blocking RAGE activity may be beneficial to patient outcome (14).

We previously described for the first time that cromolyn could block the binding of S100P with its receptor RAGE and thereby reduce the growth and invasion of pancreatic cancer in a mouse model (17). Others reported that cromolyn-induced blood clotting and increased hypoxia in a murine model of breast cancer (18) suppressed carcinogen-induced tumors in rats (19) and suppressed the growth of thyroid carcinoma (20) and pancreatic islet

Authors' Affiliations: Department of [1]Cancer Biology, [2]Experimental Therapeutics, and [3]GI Medical Oncology, UT MD Anderson Cancer Center, Houston, Texas

Note: Supplementary data for this article are available at Molecular Cancer Therapeutics Online (http://mct.aacrjournals.org/).

Corresponding Authors: Craig Logsdon, Department of Cancer Biology and Medical Oncology, UT MD Anderson Cancer Center, 1515 Holcombe Blvd, Houston, TX 77030. Phone: 713-563-3585; Fax: 713-563-8986; E-mail: clogsdon@mdanderson.org; and Thiruvengadam Arumugam, Tarumugam@mdanderson.org.

doi: 10.1158/1535-7163.MCT-12-0771

tumors (21) reportedly by blocking mast cell function. Therefore, it seems that cromolyn has at least 2 actions that are anticancer, one to inhibit mast cell secretion and one to block RAGE activation. However, despite these beneficial characteristics, cromolyn is a weak inhibitor of human mast-cell secretion and is poorly absorbed orally. For these reasons, cromolyn has never been tested clinically to determine whether it would be beneficial as a cancer therapy.

Our purpose was to design and synthesize a more potent cromolyn analog. To this end we tested several analogs. We examined the ability of analogs to affect S100P binding with its receptor RAGE and also to interfere with S100P stimulated functions *in vitro* and *in vivo*. We found that 5-methyl cromolyn (C5OH) was superior to cromolyn in each regard. These data support further development of this molecule as an anticancer agent.

Materials and Methods

Cell lines and reagents

Pancreatic cancer cell lines were obtained from American Type Tissue Collection. Cell lines were authenticated by using DNA fingerprinting (Powerplex16 System; Promega). Cells were routinely cultured in Dulbecco's Modified Eagle's Medium containing 10% FBS. Gemcitabine (Gemzar-Eli Lilly and Co.), 5-fluorouracil, taxol, and cisplatin (Sigma) were used for apoptosis study.

Synthesis of cromolyn analogs

All chemicals and solvents were obtained from Sigma-Aldrich of Fisher Scientific and used without further purification. Melting points were measured in open capillary tubes on a Buchi Melting Point B-545 apparatus and are uncorrected. ^{1}H-NMR and ^{13}C-NMR spectra were recorded on an IBM-Bruker Avance 600 (600 MHz for ^{1}H-NMR and 150.90 MHz for ^{13}C-NMR) spectrometers. Chemical shifts (δ) are determined relative to DMSO-d_6 [referenced to 2.49 ppm (δ) for ^{1}H-NMR and 39.5 ppm for ^{13}C-NMR]. Proton–proton coupling constants (J) are given in Hertz and spectral splitting patterns are designated as singlet (s), doublet (d), triplet (t), quadruplet (q), multiplet or overlapped (m), and broad (br). High-resolution mass spectra (electrospray) were acquired on an Agilent 6200 TOF system. Flash chromatography was done using Merk silica gel 60 (mesh size 230-400 ASTM) or using an Isco combiFlash Rf system with RediSep columns (normal phase silica gel (mesh size 230-400ASTM) and Fisher Optima TM grade solvents. Thin-layer chromatography (TLC) was done on E.Merk silica gel F-254 aluminum-backed plates with visualization under UV (254 nm) and by staining with potassium permanganate or ceric ammonium molybdate.

We have been synthesized cromolyn and its analogues on the basis of the known procedure described early (22) and described in the Supplementary Material. The linker 1,5-dichloropentan-3-ol was first synthesized via bubbling ethylene gas into the 3-chloropropanoyl chloride solution and the obtained ketone was further reduced to the alcohol using sodium borohydride, the synthesis of C5OH was accomplished by the condensation reaction between 2,6-dihydroxyacetophenone and 1,5-dichloropentan-3-ol using Bu_4NI, in acetone formed bis(*o*-hydroxyacetophenone) that was further condensed with an excess of diethyl oxalate and the resultant bis(2,4-dioxobutyric acid)esters were cyclized under acid condition. Then sodium salts were made by saponification of those esters with 1M NaOH solution from the corresponding disodium salt (Fig. 1B). Reagents and conditions (i) anhds. $AlCl_3$, CH_2Cl_2, 0°C, add acid chloride in 30 min, bubble ethylene gas, 5°C, 3 hours; (ii) $NaBH_4$, MeOH 0°C, 2 hours; (iii) Bu_4NI, acetone reflux, 3 days; (iv) NaOEt, EtOH, $(COOEt)_2$, 16 hours; and (vi) 1.0N NaOH, EtOH, 30 minutes.

1, 5-Dichloropentane-3-one (**2**): A suspension of anhydrous aluminum chloride (36.7 g, 0.275 mol) in DCM 150 mL was cooled to 0°C under argon. 3-Chloropropionyl chloride (**1**; 31.75 g, 0.25 mol, 24 mL, $d = 1.322$) was added dropwise with stirring for about 30 minutes. Gaseous ethylene was bubbled through the turbid suspension for about 3 hours, whereas the temperature was kept below 5°C. The clear mixture was poured into a precooled solution of concentrated hydrochloride acid (35 mL) and water (140 mL), while maintaining the temperature below 10°C throughout the process. The 2-phase mixture was stirred for about 30 minutes and the organic phase was washed with water (70 mL). After removal of the solvent, the crude product was purified by silica gel (hexane/ethylacetate 10:1) to obtain 28.9 g of 1,5-dichloropentane-3-one (75%) as a light yellow oil, which became dark red on standing in the air (storage under argon protection and in freezer was necessary).

^{1}H NMR ($CDCl_3$): δ, 3.75 (dt, $J = 2.1$, 6.3 Hz, 4H), 2.91 (dt, $J = 6.6$, 11.7 Hz, 4H).

1,5-dichloropentane-3-ol (**3**): An ice cold suspension of $NaBH_4$ (1.2 g) in MeOH (15 mL) was added drop wise to a stirred ice cooled solution of 1,5-dichloro-3-pentaneone (**2**; 9.8 g) in 60 mL of MeOH, while the temperature was kept at 0°C. The reaction mixture was stirred at this temperature for 2 hours. A total of 120 g ice was added and the mixture was extracted with dichloromethane (3 × 100 mL). The solvent was removed and the brown oily residue was dissolved in 100 mL of ether and dried over molecular sieve (4A). Removal of the solvent gave 9.9 g of light yellow oil (100%), which was used for the next step without further purification.

^{1}H NMR ($CDCl_3$): δ, 4.11 (br, 1H), 3.64 (m, 4H), 1.89 (m, 4H).

1,5-Bis(2-acetyl-3-hydroxyphenoxy)pentane-3-ol (**5**): A mixture of 2,6-dihdroxyacetophenone (**4**; 3.66 g, 24 mmol), 1,5-dichloropentane-3-ol (**3**; 1.89 g, 12 mmol), Na_2CO_3 (2.55 g, 24 mmol FW = 106), and tetrabutylammonium iodide (2.22 g, 6 mmol FW = 369) in acetone (40 mL) was heated at reflux for 3 days. The reaction mixture was checked by TLC (silica gel—hexanes/ethyl acetate = 1:1) to show 2 spot at $R_f = 0.75$ (2, 6-dihydroxyacetophenone) and 0.60 (product). After cooling down to room

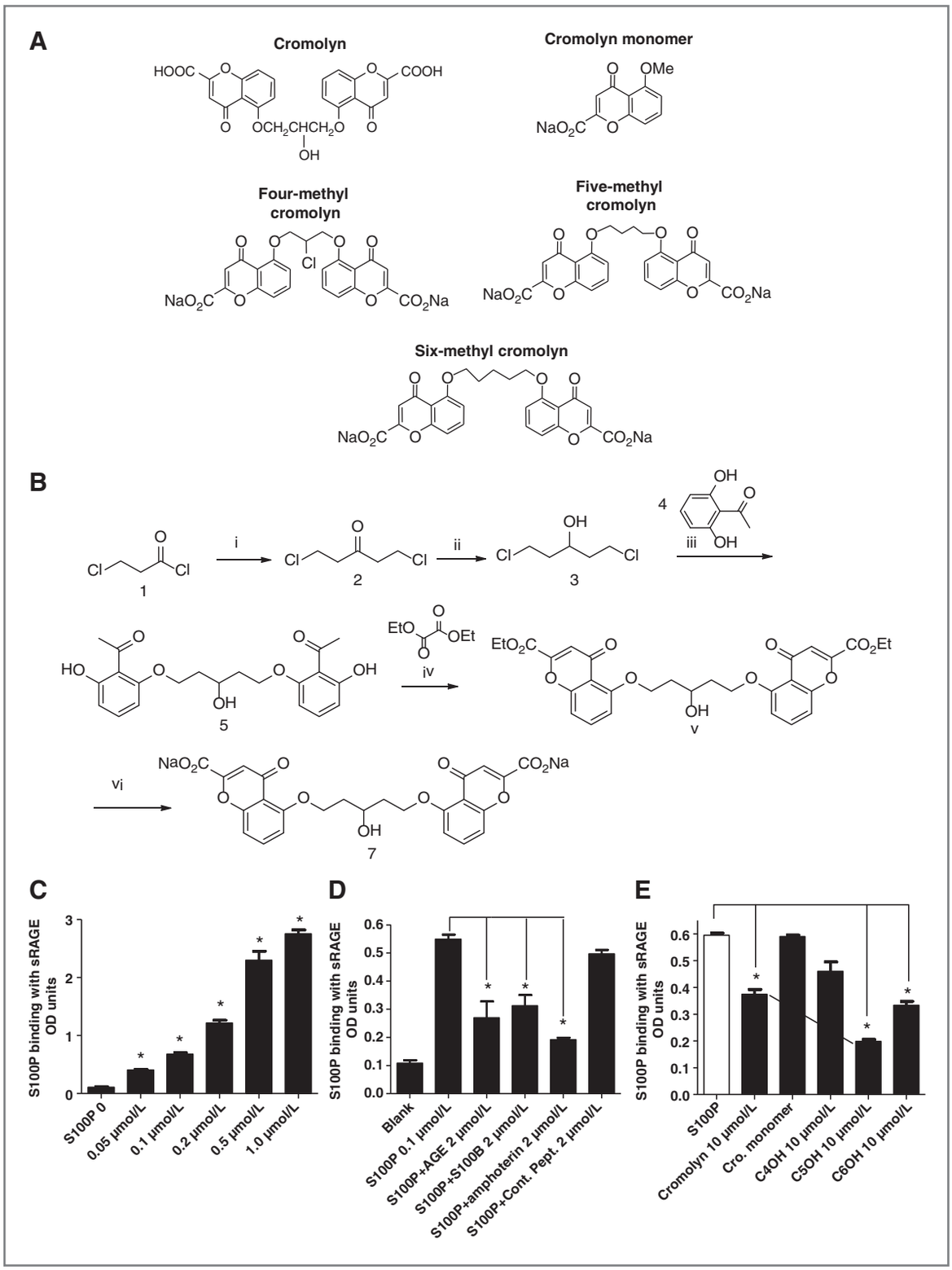

Figure 1. Cromolyn and its analogs block S100P binding with its receptor RAGE. A, chemical structure of cromolyn and its various analogs; B, synthesis of C5OH. C, S100P binds with sRAGE in ELISA-based assay, showing the specific binding between these 2 molecules (*, $P < 0.05$; $n = 3$). D, RAGE ligands (AGEs, S100B, and amphoterin), but not control peptide interfere S100P binding with RAGE by competitive binding (*, $P < 0.05$; $n = 3$). E, cromolyn and its analogs blocks S100P binding with its receptor RAGE in ELISA-based assay (*, $P < 0.05$; $n = 3$).

temperature, 10 g silica gel was added and the residue, after removing the solvent, was purified by column chromatography to obtain 1.67 g (34%) of pure 1,5-bis(2-acetyl-3-hydroxyphenoxy)pentane-3-ol as a light yellow solid along with 0.5 g (14.0%) 2,6-dihdroxyacetophenone and 1.9 g (29.0%) 1-chloro-5-(2cetyl-3-hydroxyphenoxy)pentane-3-ol with impurities.

Melting point: 157–158°C.

UV-Vis: $\lambda_{max} = 343, 279$ nm.

TLC: $R_f = 0.60$ (silica gel, hexanes/ethyl acetate = 1/1).

HPLC: $t_r = 24.3$ min (4.1 × 250 mm C18 column 10% → 80% MeCN in H2O at 1.5 mL/min over 30 minutes.

^{1}H NMR (DMSO-d_6): δ 12.1(s, 1H, 7.32 (t, $J = 8.1$ Hz, 2H), 6.57 (d, $J = 8.4$Hz, 2H), 6.48 (d, $J = 8.1$ Hz, 2H), 4.85 (d, $J = 5.7$ Hz, 1H), 4.01 (m, 4H), 3.89 (br, 1H), 1.97 (m, 2H), 1.81 (m, 2H).

^{13}C NMR (DMSO-d_6): δ 204.4, 161.0, 159.7, 135.1, 113.9, 103.8, 103.3, 66.2, 64.2, 37.1, 33.6.

Diethyl ester of 1,5-bis(2-carboxychromon-5-yloxy)) pentane-3-ol (**6**): 0.54 g Na (23 mmol) in 15 mL of ethanol was heated until all of Na was digested. To this solution, 1.8 mL (12.8 mmol) of diethyl oxalate, 1.51 g (3.9 mmol) of 1, 5-bis(2-acetyl-3-hydroxyphenoxy)propane-3-ol (**5**), and 19 mL of toluene were added at 0°C. This light yellow solution heated gently at 79°C under argon (solution became brown gradually) for 16 hours. The reaction mixture was neutralized with conc. HCl to pH 5.5 and filtered. The filtrate was vacuumed to dryness and 5 drop of conc. HCl in 5 mL of was added. The orange solution was heated to boil for about 3 minutes. The precipitate was formed, upon cooling down, which was collected by filtration to obtain 1.60 g of white solid (74%).

Melting point: 185–186°C.

UV-Vis: $\lambda_{max} = 325, 268$ nm.

TLC: $R_f = 0.45$ (silica gel, hexanes/ethyl acetate = 1/1).

HPLC: $t_r = 8.25$ min (4.1 × 50 mm C18 column 0% → 95% MeCN in H2O at 0.5 mL/min over 7.5 minutes.

^{1}H NMR (DSMO-d_6): δ 7.74 (t, $J = 8.5$ Hz, 2H), 7.20 (d, $J = 8.5$ Hz, 2H), 7.07 (d, $J = 8.5$ Hz, 2H), 6.73 (s, 2H), 5.04 (b, 1H), 4.39 (q, $J = 7$ Hz, 4H), 2.52 (dt $J = 20.0, 7.0$ Hz, 4H), 4.20 (b, 1H), 2.02 (dm, $J = 40$Hz, 4H), 1.35 (t, $J = 7.0$Hz, 6H).

^{13}C NMR (DSMO-d_6): δ 177.0, 160.5, 159.0, 157.7, 150.7, 135.9, 115.8, 114.8, 110.5, 108.9, 67.3, 66.0, 73.1, 37.4, 14.4.

Disodium salt of 1,5-bis(2-carboxychromon-5-yloxy) pentane-3-ol (**7**): To the mixture of 1,5-bis(2-carboxychromon-5-yloxy)pentane-3-ol (**6**; 2.21 g, 4 mmol) in 10 mL of ethanol was added 8 mL of 1 N NaOH at room temperature with vigorous shaking (the resultant mixture thickened and then became thinner with the addition). After the addition was complete, 10 mL of ethanol was added and the mixture was stirred for 30 minutes. The solid was filtered, washed with 10 mL of ethanol, and air-dried to obtain 1.58 g (74%) of pure disodium salt of 1,5-bis(2-carboxychromon-5-yloxy)pentane-3-ol as a white solid.

Melting point: >235°C.

UV-Vis: $\lambda_{max} = 325, 268$ nm.

TLC: $R_f = 0.50$ (silica gel, dichloromethane/methanol = 1/1).

HPLC: $t_r = 4.52$ min (4.1 × 50 mm C18 column 0% → 95% MeCN (0.1% TFA) in H2O (0.1% TFA) at 0.5 mL/min over 7.5 min.

^{1}H NMR (D_2O): δ 7.34 (t, $J = 8.5$ Hz, 2H), 6.77 (d, $J = 8.5$ Hz, 2H), 6.65 (d, $J = 8.5$ Hz, 2H), 6.40 (s, 2H), 4.06 (m, 5H), 2.05 (m, $J = 20.0, 7.0$ Hz, 4H), 4.20 (b, 1H), 2.02 (dm, $J = 40$ Hz, 4H).

^{13}C NMR (D_2O): δ 181.2, 167.8, 157.4, 157.3, 156.4, 135.5, 113.1, 112.4, 110.4, 107.8, 68.1, 66.7, 35.1.

S100P binding study

Recombinant S100P protein (13), S100P monoclonal antibody (Cat. No: 610306; R&D), and ELISA kit (KPL) were used for ELISA-based assay to determine the S100P binding affinity with its receptor RAGE. Briefly, sRAGE (5 μg/mL) was coated onto ELISA plate by using antigen-coating solution for 1 hour at room temperature, nonspecific binding sites was blocked by incubating 1% BSA solution. S100P different concentrations (0–1 μmol/L) with and without cromolyn and its various analogs were incubated in sRAGE-coated wells for 1 hour and unbound molecules were removed by wash solution. Bound S100P was detected with horseradish peroxidase–labeled anti-S100P secondary antibody and TMB (3,3′,5,5′-tetramethylbenzidene) substrate. Color development was blocked with 1 M phosphoric acid and read at 450 nm.

MTS assay

Cells were plated and allowed to adhere for 24 hours. The cells were treated with cromolyn, C5OH, and gemcitabine in different concentrations. Twenty microliters of MTS (Promega) was then added to the well and used to detect viable cells. Absorbance at 490 nm was then measured with a Micro-plate reader (MRX; Danatech Laboratory).

PI-FACS analysis

Standard propidium iodide (PI) staining by the hypotonic lysis method was used for apoptosis studies. Apoptosis was induced in 1.0×10^6 cells by treatment with gemcitabine alone or in combination with cromolyn and C5OH. After 72 hours, the cells were detached from culture dishes by incubation in 0.05% trypsin–EDTA, washed once with cold PBS, then incubated for 30 minutes in 500 μL of hypotonic solution (0.1% sodium citrate, 0.1% Triton X-100, 100 μg/mL RNase, and 50 μg/mL PI), and analyzed by flow cytometry (EPICS XL; Beckman Coulter Inc.). Cells undergoing apoptosis that had lost part of their DNA were identified as the population of cells with sub-G1 DNA content.

Luciferase assay for NF-κB activity

BxPC-3 cells stably expressing an Lenti-NF-κB-luc reporter construct were treated with S100P, cromolyn, and C5OH, or the combination for 5 hours. D-Luciferin

(150 μg/mL) was added to the cells, and luciferase activity was measured using an IVIS bioluminescence system (Caliper).

To measure NF-κB promoter activity *in vivo*, BxPC-3 cells (50,000/50 μL) stably expressing an NF-κB-luc reporter were injected orthotopically into the pancreas of 4-week-old male nude mice. After 2 weeks, mice were injected with D-luciferin [150 mg/kg body weight, intraperitoneal (i.p.) injection], and basal NF-κB activity was determined using the IVIS system. Subsequently, mice were injected with cromolyn (50 mg/kg body weight, i.p.) and C5OH (5 mg/kg body weight, i.p.), and NF-κB luciferase activity was reanalyzed after 5 hours.

Tumor growth study in syngeneic model and survival study in athymic model. All animals were maintained in a sterile environment. Cages, bedding, food, and water were all autoclaved. All animals were maintained on a daily 12-hour light/12-hour dark cycle according to the institutional animal welfare guidelines.

Syngeneic model: tumor growth and metastasis study. The antitumorigenic capability of the C5OH was assessed in 4-week-old male C57bl/6J mice by using mouse pancreatic cancer cell lines isolated from k-ras-p53$^{-/-}$ transgenic mouse tumor. Cancer cells 1×10^5/50 μL were injected into the pancreas and vehicle PBS and C5OH 5 mg/daily/i.p. were injected for another 5 weeks, at the end of the experiment tumor growth and metastasis to peritoneal cavity, spleen, and liver were analyzed by bioluminescence imaging.

Athymic model: survival study. The antitumorigenic capability and impact on survival of C5OH was studied in 4-week-old male *athymic nude* mice by using luciferase gene stably expressing highly aggressive MPanc96 cells. Luciferase-labeled Mpanc96 cells 2×10^5/50 μL were injected into the pancreas. Bioluminescent imaging was used to estimate tumor volume after 1 week and animals were divided into 4 groups of 10 animals per group, such that the mean tumor size was equal between groups. For the next 5 weeks, group I animals were treated with vehicle PBS, group II were treated with C5OH (5 mg/daily/i.p.), group III animals were treated with gemcitabine (100 mg/kg·b.w./once weekly/i.p.), and group IV were treated with combination of gemcitabine and C5OH and tumor growth was monitored. Survival was monitored for 10 weeks.

Statistical analysis

Data are presented as mean ± SE of the mean. Statistically significant differences were determined by unpaired *t* test. When more than 2 groups were analyzed ANOVA was used to analyze the data and further Newman–Keuls multiple comparison test was used to check the posttest significance. Statistical significance was defined as $P < 0.05$. Survival study was assessed overtime by observing when animals either died or became moribound to the extent that they had to be sacrificed for humane reasons. The log-rank test was used to compare survival distributions between groups. Results were compared using GraphPad Prism 4 software.

Results

C5OH is the most potent cromolyn analog for inhibition of S100P binding with RAGE

We synthesized several analogs for cromolyn (Fig. 1A and B). Our previous studies showed that S100P binds with RAGE (13, 17, 23). Therefore, in this study we designed an ELISA to assess S100P binding with RAGE. Incubation of S100P in different concentrations in sRAGE-coated wells led to dose-dependent increase in S100P binding, reflected by increased binding O.D. (Fig. 1C). To further confirm the specificity of S100P binding with sRAGE, we introduced other RAGE ligands AGE (2 μmol/L), S100B (2 μmol/L), and amphoterin (2 μmol/L) with S100P (0.1 μmol/L). Each of these known RAGE ligands led to reduced binding of S100P with sRAGE, confirming the specificity of ligand–receptor interaction in this ELISA (Fig. 1D).

Next, we introduced 10 μmol/L concentrations of cromolyn, or cromolyn monomer, cromolyn 4 methyl (C4), cromolyn 5 methyl (C5), and cromolyn 6 methyl (C6) compounds along with S100P (0.1 μmol/L; Fig. 1E). As expected, cromolyn blocked the binding of S100P with sRAGE and reduced binding capacity to 40%. In contrast, cromolyn monomer and C4 compounds did not affect S100P binding with sRAGE. However, C5OH and C6OH both blocked the binding of S100P with RAGE. In comparison, C5OH blocked S100P binding to a greater extent than did cromolyn (40% vs. 65%) whereas C6OH did not inhibit significantly greater than cromolyn ($P < 0.05$).

To assess the potency of C5OH, we determined the concentration at which it was as effective at inhibiting S100P binding to RAGE as compare with cromolyn. For this purpose we incubated different concentrations of cromolyn or C5OH along S100P (0.1 μmol/L) in sRAGE-coated plates. Cromolyn caused a dose-dependent inhibition of S100P binding and a maximal dose of 10 μmol/L blocked 40% of total binding. C5OH also caused a dose-dependent inhibition if S100P binding. However, this inhibition occurred lower concentrations and at a dose of 1 μmol/L C5OH inhibited 65% of S100P binding (Fig. 2A). Inhibition by C5OH at 100 nmol/L inhibited to the same extent as cromolyn at 10 μmol/L. Thus, C5OH is roughly 100 times as potent as its parent molecule, cromolyn, on inhibiting S100P binding with its receptor RAGE.

C5OH was more effective at inhibiting RAGE-mediated NF-κB activity, cell growth, and apoptosis than other cromolyn analogs

In our previous study we showed that extracellular addition of S100P activates NF-κB in PDAC cells (17). In this study we used this assay to analyze the relative efficiency of C5OH. Therefore, we added 0.1 μmol/L concentration of S100P with and without cromolyn or C5OH to NF-κB reporter cells (Fig. 2B). As was observed

in the binding study, C5OH inhibited S100P-induced NF-κB activity to a greater extent and at a 10-time lower concentration than cromolyn (Fig. 2B).

One of the most clinically relevant effects of cromolyn that we reported previously was its ability to increase the effectiveness of gemcitabine to kill PDAC cells (17). Therefore, we also examined whether C5OH could perform as well or better than cromolyn in this assay. For this investigation we examined the effects of including either 10 μmol/L concentration of cromolyn or 1 μmol/L concentration of C5OH in combination with gemcitabine (1 μmol/L) on the PDAC cell line BxPC-3. We found that C5OH was as effective at 1/10th the concentration as was cromolyn at increasing the reduction of cell numbers induced by gemcitabine (Fig. 2C) Similarly, C5OH increased the percentage of gemcitabine induced apoptotic cells to an extent at least as great as did cromolyn but at 1/10th the concentration (Fig. 2D).

C5OH enhanced gemcitabine-induced apoptosis in the BxPc-3 cell line, which is a relatively sensitive cell for chemotherapeutic drugs. To examine the effectiveness of C5OH in a more resistant PDAC cell line, we selected Mpanc96 cells, which are highly resistant to gemcitabine and also to other chemotherapeutic drugs. The combination of C5OH along with the common cytotoxic drugs gemcitabine, cisplatin, and 5-fluouracil enhanced the induction of apoptosis (Fig. 2E). In contrast, C5OH did not improve the effectiveness of taxol, which employs a

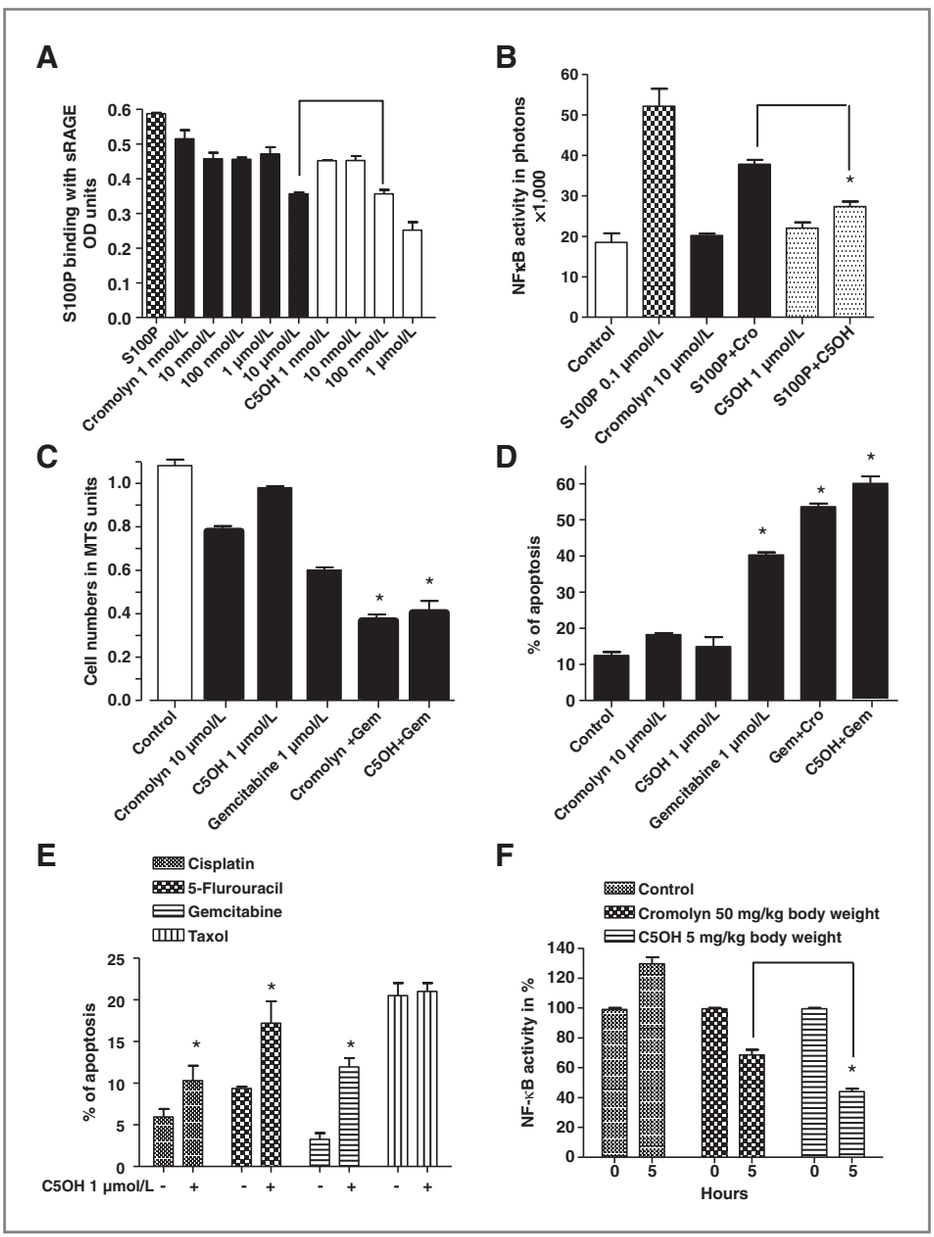

Figure 2. C5OH blocks S100P-mediated functions better than cromolyn. A, analog of cromolyn, C5OH (100 nmol/L) blocks binding of S100P with its receptor RAGE in 100 times lesser concentration than parent molecule cromolyn (10 μmol/L), showing the better potency (*, $P < 0.05$; $n = 3$). B, C5OH blocks S100P-induced NF-κB activity in 10 times lesser concentration than parent molecule cromolyn, showing better potency. C–D, C5OH improved gemcitabine efficiency by reducing cell growth and increasing apoptosis in 10 times lesser concentration than parent molecule cromolyn, showing better potency (*, $P < 0.05$; $n = 3$). E, C5OH sensitized drug-resistant pancreatic cancer cells to various chemotherapeutic drugs, showing the better clinical use (*, $P < 0.05$; $n = 3$). F, *in vivo* C5OH treatment reduced NF-κB activity better than cromolyn at a 10 times lesser concentration, showing better efficacy *in vivo* (*, $P < 0.05$).

different mechanism of action. Because some PDAC cells undergo autophagy rather than apoptosis, we repeated the same study by quantifying viable cells using MTS reagent and we observed the same trend of result. This further confirms C5OH enhance cisplatin, 5FU, and gemcitabine effect but not Taxol (data not shown). The same trend of result was observed in another drug-resistant cell line MiaPaCa-2 (data not shown).

To determine if C5OH would also be superior to cromolyn at inhibiting RAGE activation *in vivo*, we monitored the level of NF-κB activity in PDAC reporter cells using the IVIS bioluminescence system, as we have reported previously (17). Nude mice-bearing tumors formed from NF-κB reporter cells were injected with either cromolyn (50 mg/kg·b.w./i.p.) or C5OH (5 mg/kg·b.w./i.p.) and NF-κB–generated luciferease activity was measured after 5 hours. We observed that a 10 times lesser concentration of C5OH compound inhibited NF-κB activity to a greater extent than did its parent compound cromolyn (Fig. 2F).

C5OH inhibits pancreatic cancer growth, metastasis, and prolongs survival to a greater extent than cromolyn in preclinical mouse models

After we confirmed that C5OH was effective *in vivo* on NF-κB activity, we analyzed its effects on tumor growth and metastasis. Apart from effects of cromolyn on S100P-mediated functions, it is also potent mast cell blocker. To test the effects of inhibiting both mast cells and RAGE activation, we analyzed the effects of C5OH on tumor growth and metastasis in immune system intact syngenic model. Mouse PDAC cells lines isolated from K-ras transgenic animals were injected into genetically identical C57 animals and after tumor growth was established we injected C5OH (5 mg/kg·b.w./i.p.). Treatment with C5OH drastically reduced primary tumor growth and metastasis (Fig. 3A–C). Treatment with C5OH did not alter the body weight of the animals, proving the lack of toxicity.

Next, we developed an aggressive PDAC xenograft model by injecting Mpanc96 PDAC cells orthotopically into the pancreas of nude animals. These animals were separated into 4 groups: first group received PBS-vehicle treatment, second group was treated with C5OH (5 mg/kg·b.w./i.p.) alone, third group was treated with gemcitabine (100 mg/kg·b.w./week/i.p.) alone, and the fourth group received both C5OH and gemcitabine. We observed that C5OH significantly reduced tumor growth and increased animal survival (Fig. 4A and B). Gemcitabine either alone or in combination with C5OH was ineffective in this model.

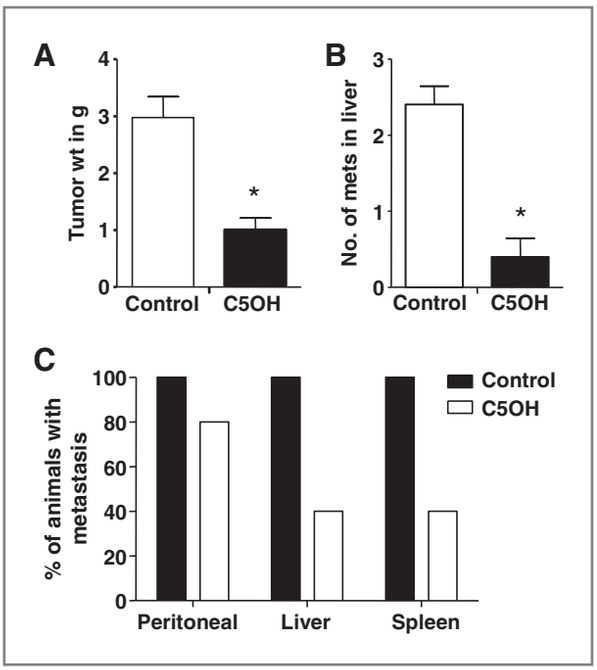

Figure 3. C5OH treatment reduces PDAC tumor growth and metastasis in syngeneic model. Treatment of C57 black immune competent animals with C5OH (5 mg/kg·b.w./i.p.) reduced mouse PDAC tumor growth (A) and metastasis to liver, spleen, and peritoneal cavity (B–C) in syngeneic model (*, $P < 0.05$).

Discussion

Many earlier studies have suggested that both genetic and epigenetic alterations lead to the aggressive nature of PDAC (5, 24–26). S100P is one of the oncogenic molecules whose expression has been described both in PDAC and many different cancers, and that is associated with drug resistance, metastasis, and poor clinical outcome (7–9). S100P is secreted from the cancer cells and acts by binding and activating RAGE leading to key signaling events such as activation of MAPkinase and NF-κB (13). Blocking S100P function in preclinical models reduced tumor growth (7, 17, 27, 28) and metastasis (17, 23) and also reversed drug resistance (17). Taken together, these data suggest that S100P is a promising therapeutic target. Our study clearly showed that C5OH blocked the S100P-mediated growth and antiapoptotic effect in PDAC and improved the animal survival.

We previously described that the small molecule cromolyn, which is widely used to treat allergic symptoms, bound S100P and prevented its activation of RAGE (17). We observed that cromolyn inhibited pancreatic cancer cell function *in vitro* and that this was mediated by interference with S100P and RAGE. However, the effects of cromolyn *in vivo* on pancreatic tumor growth and metastasis was even greater than expected from the *in vitro* data (17, 29). The likely explanation is that *in vivo* cromolyn is also affecting tumors through second mechanisms. Cromolyn is known as an inhibitor of mast cell secretion (30). Mast cells are important inflammatory cells that participate in immune responses during allergic reactions (30). Furthermore, recent studies suggest that these cells also participates cancers (31–38). We found that in the spontaneous mouse model of PDAC [K-ras (G12V)], there was an early influx of mast cells to the tumor

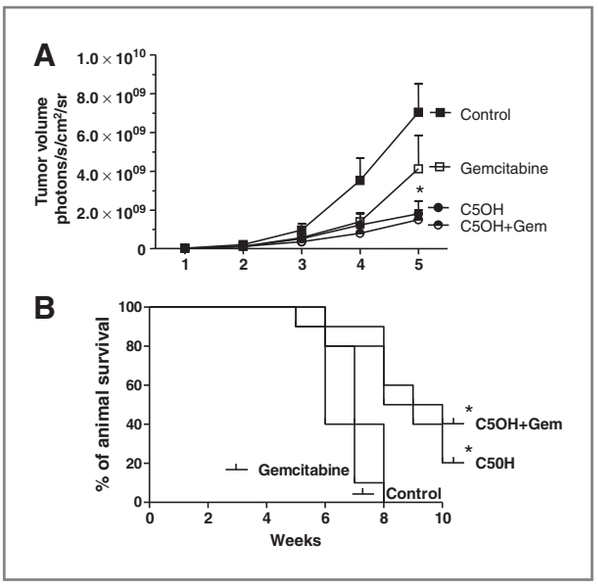

Figure 4. C5OH treatment reduces PDAC tumor growth and improved survival. *In vivo* treatment C5OH (5 mg/kg·b.w./i.p.) reduced tumor growth (A) and increased the survival (B) of animals either alone [log-rank (Mantel–Cox) test, $P < 0.003$; median survival control 6 weeks vs. C5OH 9.5 weeks] or along with gemcitabine [log-rank (Mantel–Cox) test, $P < 0.04$; gemcitabine 7 week vs. C5OH + Gem 8.5 weeks; *, $P < 0.05$].

microenvironment (31). Furthermore, PDAC tumor growth was suppressed in mast cell–deficient Kit(w-sh/w-sh) mice, but aggressive PDAC growth was restored when PDAC cells were injected into mast cell–deficient mice reconstituted with wild-type bone marrow–derived mast cells. We also found that mast cell infiltration into the tumor microenvironment was predictive of poor prognosis in patients with PDAC (33). Therefore, mast cells are likely second mechanisms whereby cromolyn reduces tumor aggressiveness.

Cromolyn or its analog may be extremely beneficial in cancer. Epidemiological studies have revealed that prolonged use of nonsteroidal antiinflammatory drugs (NSAIDs) reduces the risk of cancer as well as tumor growth in animal models. However, an experimental study showed that upregulation of S100P expression by NSAIDs negatively affects the antitumorigenic activity of NSAIDs through inhibition of apoptosis, stimulation of cancer cell growth, and invasion. This explains the recent observation in gastric cancer cells, that either silencing of S100P or cromolyn treatment improved the effect of celecoxib (38). Taken together, the evidence is strong that cromolyn or its analogs would have many beneficial effects. Compare with cromolyn our novel compound C5OH strongly inhibited the S100P functions. An analog with a similar structure was also found to be superior to cromolyn for inhibition of mast cell secretion (22).

In summary, cromolyn is a useful therapeutic against cancer as it can block both the tumorigenic ability of S100P interaction with RAGE and the cancer promoting influences of mast cell functions. Our novel cromolyn analog C5OH is more potent and efficacious than cromolyn. This molecule should find multiple uses in clinical practice.

Disclosure of Potential Conflicts of Interest

No potential conflicts of interest were disclosed.

Authors' Contributions

Conception and design: T. Arumugam, W.G. Bornmann, C.D. Logsdon
Development of methodology: T. Arumugam, C.D. Logsdon
Acquisition of data (provided animals, acquired and managed patients, provided facilities, etc.): V. Ramachandran, C.D. Logsdon
Analysis and interpretation of data (e.g., statistical analysis, biostatistics, computational analysis): T. Arumugam, V. Ramachandran, D. Maxwell, C.D. Logsdon
Writing, review, and/or revision of the manuscript: T. Arumugam, V. Ramachandran, C.D. Logsdon
Study supervision: C.D. Logsdon

Grant Support

This work was supported in part by the Lockton Endowment and by the Public Health Service Grant DK56338 to C.D. Logsdon, which funds the Texas Medical Center Digestive Diseases Center.

The costs of publication of this article were defrayed in part by the payment of page charges. This article must therefore be hereby marked *advertisement* in accordance with 18 U.S.C. Section 1734 solely to indicate this fact.

Received July 24, 2012; revised December 17, 2012; accepted January 2, 2013; published OnlineFirst January 9, 2013.

References

1. Raimondi S, Maisonneuve P, Lowenfels AB. Epidemiology of pancreatic cancer: an overview. Nat Rev Gastroenterol Hepatol 2009;6:699–708.
2. Jemal A, Siegel R, Xu J, Ward E. Cancer statistics, 2010. CA Cancer J Clin 2010;60:277–300.
3. Assifi MM, Lu X, Eibl G, Reber HA, Li G, Hines OJ. Neoadjuvant therapy in pancreatic adenocarcinoma: a meta-analysis of phase II trials. Surgery 2011;150:466–73.
4. Nieto J, Grossbard ML, Kozuch P. Metastatic pancreatic cancer 2008: is the glass less empty? Oncologist 2008;13:562–76.
5. Zavoral M, Minarikova P, Zavada F, Salek C, Minarik M. Molecular biology of pancreatic cancer. World J Gastroenterol 2011;17:2897–908.
6. Becker T, Gerke V, Kube E, Weber K. S100P, a novel Ca(2+)-binding protein from human placenta. cDNA cloning, recombinant protein expression and Ca2+ binding properties. Eur J Biochem 1992;207:541–7.
7. Arumugam T, Logsdon CD. S100P: a novel therapeutic target for cancer. Amino Acids 2011;41:893–9.
8. Logsdon CD, Simeone DM, Binkley C, Arumugam T, Greenson JK, Giordano TJ, et al. Molecular profiling of pancreatic adenocarcinoma and chronic pancreatitis identifies multiple genes differentially regulated in pancreatic cancer. Cancer Res 2003;63:2649–57.
9. Guerreiro Da Silva ID, Hu YF, Russo IH, Ao X, Salicioni AM, Yang X, et al. S100P calcium-binding protein overexpression is associated with immortalization of human breast epithelial cells *in vitro* and early stages of breast cancer development *in vivo*. Int J Oncol 2000;16:231–40.
10. Fuentes MK, Nigavekar SS, Arumugam T, Logsdon CD, Schmidt AM, Park JC, et al. RAGE activation by S100P in colon cancer stimulates

growth, migration, and cell signaling pathways. Dis Colon Rectum 2007;50:1230–40.
11. Mousses S, Bubendorf L, Wagner U, Hostetter G, Kononen J, Cornelison R, et al. Clinical validation of candidate genes associated with prostate cancer progression in the CWR22 model system using tissue microarrays. Cancer Res 2002;62:1256–60.
12. DiNorcia J, Lee MK, Moroziewicz DN, Winner M, Suman P, Bao F, et al. RAGE gene deletion inhibits the development and progression of ductal neoplasia and prolongs survival in a murine model of pancreatic cancer. J Gastrointest Surg 2012;16:104–12
13. Arumugam T, Simeone DM, Schmidt AM, Logsdon CD. S100P stimulates cell proliferation and survival via receptor for activated glycation end products (RAGE). J Biol Chem 2004;13:5059–65.
14. Logsdon CD, Fuentes MK, Huang EH, Arumugam T. RAGE and RAGE ligands in cancer. Curr Mol Med 2007;7:777–89.
15. Mebratu Y, Tesfaigzi Y. How ERK1/2 activation controls cell proliferation and cell death: is subcellular localization the answer? Cell Cycle 2009;15:1168–75.
16. Pan X, Arumugam T, Yamamoto T, Levin PA, Ramachandran V, Ji B, et al. Nuclear factor-kappaB p65/relA silencing induces apoptosis and increases gemcitabine effectiveness in a subset of pancreatic cancer cells. Clin Cancer Res 2008;14:8143–51.
17. Arumugam T, Ramachandran V, Logsdon CD. Effect of cromolyn on S100P interactions with RAGE and pancreatic cancer growth and invasion in mouse models. J Natl Cancer Inst 2006;98:1806–18.
18. Samoszuk M, Corwin MA. Mast cell inhibitor cromolyn increases blood clotting and hypoxia in murine breast cancer. Int J Cancer 2003;107: 159–63.
19. Ionov ID. Influence of inhibitor of mast-cell activity on carcinogenesis in rats. Int J Cancer 1988;41:777–8.
20. Melillo RM, Guarino V, Avilla E, Galdiero MR, Liotti F, Prevete N, et al. Mast cells have a protumorigenic role in human thyroid cancer. Oncogene 2010;29:6203–15.
21. Soucek L, Lawlor ER, Soto D, Shchors K, Swigart LB, Evan GI. Mast cells are required for angiogenesis and macroscopic expansion of Myc-induced pancreatic islet tumors. Nat Med 2007;13:1211–8.
22. Cairns H, Fitzmaurice C, Hunter D, Johnson PB, King J, Lee TB, et al. Synthesis and structure-activity relationships of disodium cromoglycate and some related compounds. J Med Chem 1972;15:583–9.
23. Arumugam T, Simeone DM, Van Golen K, Logsdon CD. S100P promotes pancreatic cancer growth, survival, and invasion. Clin Cancer Res 2005;11:5356–64.
24. Bradley CJ, Yabroff KR, Dahman B, Feuer EJ, Mariotto A, Brown ML. Productivity costs of cancer mortality in the United States: 2000–2020. J Natl Cancer Inst 2008;100:1763–70.
25. Saif MW. Pancreatic neoplasm in 2011: an update. JOP 2011;12: 316–21.
26. Wang Z, Ali S, Banerjee S, Bao B, Li Y, Azmi AS, et al. Activated K-Ras and INK4a/Arf deficiency promote aggressiveness of pancreatic cancer by induction of EMT consistent with cancer stem cell phenotype. J Cell Physiol 2013;228:556–62.
27. Whiteman HJ, Weeks ME, Dowen SE, Barry S, Timms JF, Lemoine NR, et al. The role of S100P in the invasion of pancreatic cancer cells is mediated through cytoskeletal changes and regulation of cathepsin D. Cancer Res 2007;67:8633–42.
28. Basu GD, Azorsa DO, Kiefer JA, Rojas AM, Tuzmen S, Barrett MT, et al. Functional evidence implicating S100P in prostate cancer progression. Int J Cancer 2008;123:330–9.
29. Kim CE, Lim SK, Kim JS. *In vivo* antitumor effect of cromolyn in PEGylated liposomes for pancreatic cancer. J Control Release 2012;157:190–5.
30. Theoharides TC. Mast cells and pancreatic cancer. N Engl J Med 2008;358:1860–1.
31. Chang DZ, Ma Y, Ji B, Wang H, Deng D, Liu Y, et al. Mast cells in tumor microenvironment promotes the *in vivo* growth of pancreatic ductal adenocarcinoma. Clin Cancer Res 2011;17: 7015–23.
32. Gilfillan AM, Austin SJ, Metcalfe DD. Mast cell biology: introduction and overview. Adv Exp Med Biol 2011;716:2–12.
33. Beer TW, Ng LB, Murray K. Mast cells have prognostic value in Merkel cell carcinoma. Am J Dermatopathol 2008;30:27–30.
34. Elpek GO, Gelen T, Aksoy NH, Erdoğan A, Dertsiz L, Demircan A, et al. The prognostic relevance of angiogenesis and mast cells in squamous cell carcinoma of the oesophagus. J Clin Pathol 2001; 54:940–4.
35. Molin D, Edström A, Glimelius I, Glimelius B, Nilsson G, Sundström C, et al. Mast cell infiltration correlates with poor prognosis in Hodgkin's lymphoma. Br J Haematol 2002;119:122–4.
36. Esposito I, Menicagli M, Funel N, Bergmann F, Boggi U, Mosca F, et al. Inflammatory cells contribute to the generation of an angiogenic phenotype in pancreatic ductal adenocarcinoma. J Clin Pathol 2004;57:630–6.
37. Strouch MJ, Cheon EC, Salabat MR, Krantz SB, Gounaris E, Melstrom LG, et al. Crosstalk between mast cells and pancreatic cancer cells contributes to pancreatic tumor progression. Clin Cancer Res 2010;16:2257–65.
38. Namba T, Homan T, Nishimura T, Mima S, Hoshino T, Mizushima T. Up-regulation of S100P expression by non-steroidal anti-inflammatory drugs and its role in anti-tumorigenic effects. J Biol Chem 2009; 284:4158–67.